

Quantifying spatial homogeneity of urban road networks via graph neural networks

Authors

Jiawei Xue¹, Nan Jiang², Senwei Liang³, Qiyuan Pang³, Satish V. Ukkusuri^{1,*}, Jianzhu Ma^{2,*}

Affiliations

¹Lyles School of Civil Engineering, Purdue University, West Lafayette, IN 47907, USA.

²Department of Computer Science, Purdue University, West Lafayette, IN 47907, USA.

³Department of Mathematics, Purdue University, West Lafayette, IN 47907, USA.

*Corresponding author. Email: sukkusur@purdue.edu (S.V.U.) majianzhu@purdue.edu (J.M.)

Abstract

The spatial homogeneity of an urban road network (URN) measures whether each distinct component is analogous to the whole network and can serve as a quantitative manner bridging network structure and dynamics. However, given the complexity of cities, it is challenging to quantify spatial homogeneity simply based on conventional network statistics. In this work, we use Graph Neural Networks to model the 11,790 URN samples across 30 cities worldwide and use its predictability to define the spatial homogeneity. The proposed measurement can be viewed as a non-linear integration of multiple geometric properties, such as degree, betweenness, road network type, and a strong indicator of mixed socio-economic events, such as GDP and population growth. City clusters derived from transferring spatial homogeneity can be interpreted well by continental urbanization histories. We expect this novel metric supports various subsequent tasks in transportation, urban planning, and geography.

INTRODUCTION

Globally, road networks have sprawled due to rapid urbanization over the past decades, especially in developing countries. The urban road network (URN) plays a central role in cities to allow for people connectivity¹ and goods movement. URNs are complex due to their interdependence with population, infrastructure facilities², and other urban transport modes³. Despite their complexity, there are underlying signatures that reveal the interplay between the structure and functionality (such as network dynamics^{4,5}, traffic congestion^{6,7}, land use⁸). At an aggregate level, the most common features used to study the URN are the “scaling laws”^{4,9,10}, which suggest universal mechanisms of road networks. Other urban scientists also exploited a variety of topology features, such as road length distribution¹⁰, relative angle¹¹, degree distribution^{12,13}, betweenness centrality^{14,15}, clustering coefficient¹⁶, block shape¹⁷, and travel routes morphology¹⁸. However, different types of “scaling laws” describe URN from a global perspective and thus often do not have the resolution to reserve the local network details such as a particular city region. Another drawback is that conventional network metrics only provide the statistics from nodes, links, blocks, and paths, omitting the multi-scale paradigm of URN thereby limiting their versatility in road network design, cascade failure analysis, and road planning. Given these deficiencies, there is a need for developing systematic network models and metrics that consider the non-linear structural interdependencies of URNs at both the micro- and macro-level.

Spatial homogeneity of a URN, based on Fractal theory¹⁹, evaluates whether the local structure of each distinct unit is analogous to the whole system in terms of the topological pattern. Accordingly, messy-planned URN with irregular-shape intersections, non-uniform blocks would have low spatial homogeneity while carefully planned URN with well-organized intersections and blocks have high spatial homogeneity. URN spatial homogeneity encodes the “local network” from neighborhood contexts, and compares it with the general pattern of the “whole network”, which is derived from non-linear interaction mining. It is typically hard to measure spatial homogeneity because (1) both the short- and long-range local road connections, which embody intuitive road network features that residents perceive during daily communications, should be captured; (2) topological patterns of URN are diverse and may not be distributed uniformly on space, causing difficulty in detecting a global pattern; (3) a linear mathematical equation is insufficient to integrate multiple structural features from distinct aspects such as degree, betweenness, and clustering coefficient because URN is indeed a non-linear dynamic system.

Addressing these restrictions necessitates an advanced data-driven approach capturing the multi-scale and non-linear properties in complex road networks. “Scale laws” and conventional network features (such as degree, neighborhood, shortest path) are incompetent here because they only describe the road network from a fixed-scale perspective. The modeling challenge can be overcome by an innovative network modeling technique, Graphical Neural Networks (GNN), which is a recursive version of deep neural networks and has achieved tremendous success in branches of graph-based employments, such as drug discovery²⁰, social friendship prediction^{21,22}, human mobility computation²³, and visual question answering²⁴. The short- and long-range local message passing mechanism and non-linear layers in GNN provide a convenient way to capture the nonlinearity in complicated URN geometry from a multi-scale perspective²⁵. In this work, we claim there is a fundamental connection between the spatial homogeneity of URN and the predictability of GNN models, as they both measure the topology similarity between subnetworks and the whole network under levels of granularity.

Using the predictability of a machine learning model to characterize a system has many pioneering applications. For instance, epidemiologists leveraged the accuracy of the epidemic prediction to identify the airline network properties in determining the global disease diffusion pattern²⁶. Ecologists also found the complexity of an ecosystem could be well reflected by the performance of various machine learning tasks, such as identifying the driver species and tracing the habitat of threatened birds²⁷. For urban scientists, the predictability of the GNN model is promising to fill the research gap between the road network structure and dynamics, based on successful application of Fractal theory in percolation problems²⁸. For a few years, betweenness has been regarded as an approximation of network flow^{29,30} but it is shown to be invariant across cities¹⁵ and has a relatively weak correlation with traffic flow computed from GPS data³¹. GNN predictability is also expected to numerically explain other road network structural features such as the novel classification of “densification roads” and “exploration roads”³² during urban sprawl period, providing additional support for URN evaluation and planning.

In this work, we train GNN models to predict the road connections on the testing URN samples from 30 cities in the United States, Europe, and Asia, and use the F1 score to investigate the relationship between spatial homogeneity and existing network metrics as well as socio-economic factors. Specifically, we collect the URN data from the OpenStreetMap³³ and perform the node-merging to replicate intersections (**Methods**). The performance is evaluated by predicting the 20% of the roads in each city hidden for tests. Extensive experiments demonstrate that Relational-GCN (R-GCN) accomplishes a better prediction performance than other models on the 30 major cities. We use the F1 score from R-GCN to represent the spatial homogeneity of the URN and find strong correlations between spatial homogeneity and (1) URN type compositions; (2) SNDi (Street-Network Disconnectedness index)³⁴. We further examine 15 measures from 4 topological and social-economic aspects and report statistically significant interactions between spatial homogeneity and degree, betweenness, GDP and population growth. To explore the inter-city URN homogeneity, we establish a City Homogeneity Transfer Matrix (CHTM) by measuring the transferability of predictions among distinct cities. Results suggest that city clusters are highly consistent with the region (USA, Europe, Asia) while the transferring F1 scores can be well interpreted using road network “diversity”. CHTM reveals profound global inheritance and development patterns of road networks that are invisible to “scaling laws” or any previous network metric.

RESULTS

Using GNN to model URN

We utilize a graph to model a URN, in which road intersections and road segments were denoted by nodes and edges, respectively (**Fig. 1a**). The problem we address is a “link prediction” problem in machine learning^{35,36}, where we predict the presence of an edge based on the structural roles of its two endpoints. The intuition of selecting this task was that a URN with high spatial homogeneity is likely to contain a lot of edges that are able to be recovered by the rest of the graph. To construct our computational framework, we collected 11,790 URN data from 30 cities in the USA, Europe and Asia (**Supplementary Tables 1-3**). We used a node merging algorithm to remove the duplicate intersections from the raw data (**Methods**). The road network data was fed into a R-GCN model³⁷ to generate a low dimensional representation (embedding) for each node, which was a non-linear aggregation of its neighbors’ representation through a neural network (**Fig. 1b**). Next, we adopted a two-sided projection function, named DistMult³⁸, to transform the representations of a pair of nodes into their connecting strength and then used a fixed threshold to determine the final prediction (**Fig. 1c**). The weights of R-GCN and DistMult were jointly trained in an end-to-end manner on the training URN samples within the same city. To further fit our model to this task, we also implemented R-GCN*, which appended two minor decoding improvements to original R-GCN, to avoid “acute angles” and “intersecting links” in the predictions (**Methods**). To the best of our knowledge, there is no other publicly available approach performing similar approaches to predict links on a URN. Therefore, to benchmark our R-GCN model, we explored and implemented five other GNN variants (**Methods**).

As “link prediction” is a highly imbalanced machine learning task (more negative data than positive data), we evaluated the prediction performance using both the area under the precision-recall curve (AUPRC) and F1 score which was a weighted average of precision and recall. Overall, the R-GCN* achieved a prediction performance with AUPRC=0.28 and F1 score=0.42 (**Fig. 1d**), and outperformed the second-best model by 0.12 (AUPRC of R-GCN=0.16), demonstrating the power of R-GCN* in capturing the link existence in a URN. The consistent superiority of R-GCN* and R-GCN were also exhibited in the testing samples when evaluated based on the continents of the cities (i.e., USA, Europe, and Asia) (**Figs. 1e-g**). The performance illustrated large variance across different cities with a maximum of 0.690 (Chicago) and a minimum of 0.199 (Stockholm). We also assessed the link prediction performance using the area under the receiver-operating curve (AUROC) (**Supplementary Fig. 6**) and demonstrated that AUROC reached 0.96 for R-GCN which still outperformed other GNN variants by a margin of at least 0.02 (AUROC of GraphSage=0.94). Since all models only provided the connecting strength for each pair of nodes, we defined the sigmoid connecting strength threshold as 0.61 by maximizing the F1 score in the best model, R-GCN*. That is to say, if the sigmoid connecting strength for two nodes (intersections) is at least 0.61, then we claim they are joined by a road segment in the real world, because their “roles” are similar in the road network.

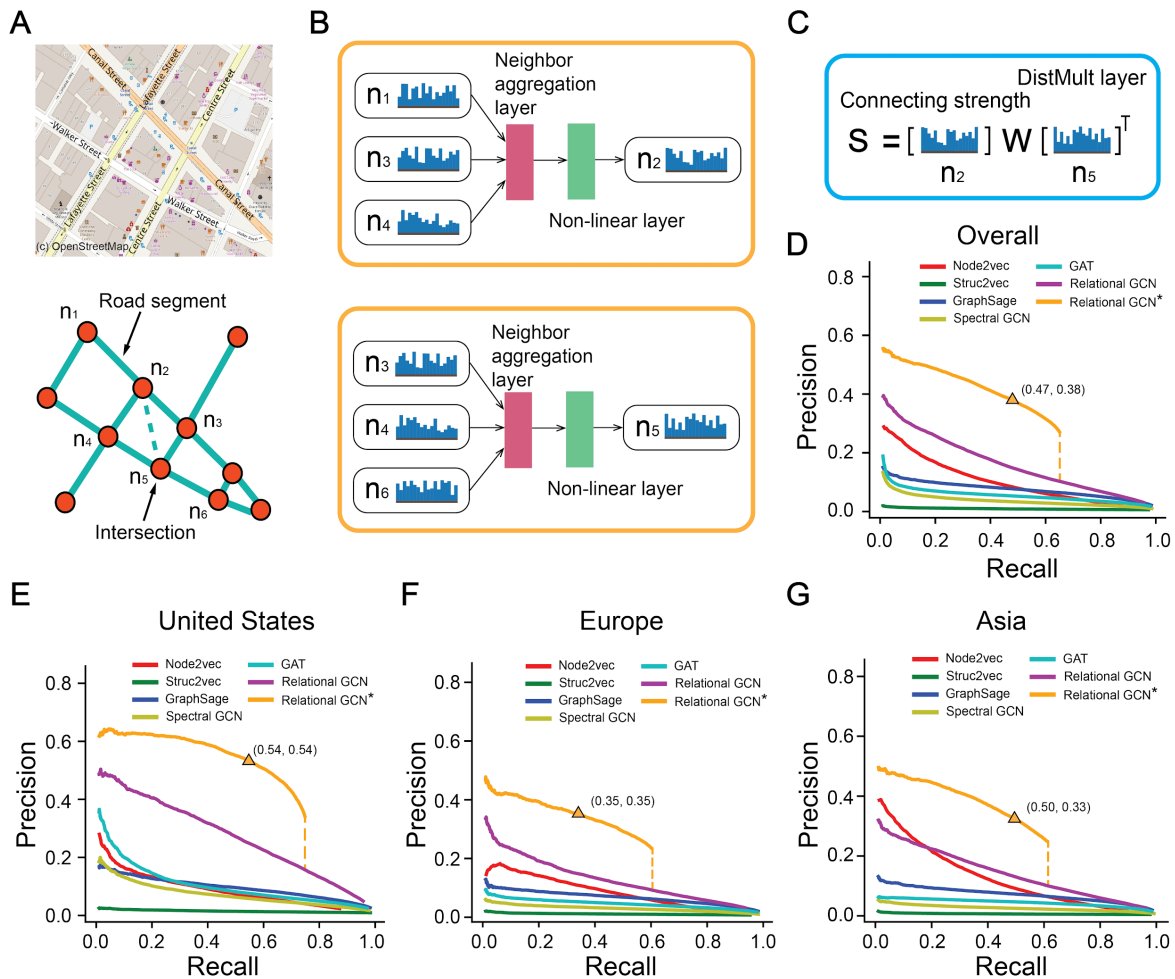


Fig. 1. Road network prediction procedure. (A) A road network in Manhattan, New York. **(B)** Message-passing mechanism between two layers of graph neural networks. The node embeddings of nodes 2 and 5 are non-linear aggregations of their neighborhood nodes' embeddings (nodes 1, 3, 4, nodes 3, 4, 6) in the lower layer. **(C)** Definition of connecting strength by DistMult. It is calculated by a weighted dot product of the final embeddings of two endpoint nodes (W is a diagonal matrix). **(D)** Precision-recall curves of the binary link prediction for testing URN samples. **(E), (F), (G)** Precision-recall curves for testing URN samples in the United States, Europe, and Asia.

Associations with URN types and SNDi

We hypothesize that the predictability of different cities capture the inherent properties of the road network designs. We adopt the F1 score of our prediction to indicate the spatial homogeneity of a URN because it demonstrates reasonable connections with multiple geographic properties of a URN. Using the *k*-means algorithm, we clustered the 11,790 URN from 30 cities into 4 types based on 11 measurements^{34,39} of simple network statistics (**Fig. 2a, Methods**). The selected 11 network metrics fell into the categories of node degree, circuitry, and dendricity (**Supplementary Table 6**). **Fig. 2a** showed that Type 1 URN had the largest average degree (3.11, Types 2 to 4: 2.78, 2.64, 2.60) and the largest fraction of “Degree \geq 4” nodes (37.8%, Types 2 to 4: 19.6%, 20.6%, 17.0%). Type 2 URN was characterized by a large proportion of “Degree=3” nodes (47.7%, Types 1, 3, 4: 41.2%, 41.5%, 40.6%). The key features defining Type 3 were the “Degree=1” nodes and dead-end edges. Type 4 stood out owing to the largest values of circuitry and fraction of bridges. Based on the dominant features of each type, we nominated Types 1 to 4 as “Grid”, “Degree-3”, “Irregular-grid”, and “Circuitous”, respectively (see **Tables 7-10** and **Supplementary Fig. 7** for 48 real instances in different cities and center points of these types).

Afterwards, we interpreted the discrepancy of F1 score distribution across distinct cities (**Fig. 2b**) from the road network type perspective. For all the testing samples, there were significant performance disparities across these 4 types of the URN (**Fig. 2c**). In particular, the F1 score associated with “Grid” URN (average: 0.526) was significantly larger than “Degree-3”, “Irregular-grid”, “Circuitous” (average: 0.413, 0.341, 0.314) with P -values $<1.0e-37$ under one-sided t-test, suggesting the more predictable patterns or city regions existing in “Grid” type. We thus hypothesized that a city with a large proportion of “Grid” URN could have high predictability. To test the hypothesis, we calculated the URN type composition for each city (**Fig. 2d, Supplementary Fig. 8**). As expected, the average F1 score of a city was positively correlated with the proportions of “Grid” (Pearson correlation=0.702). Another interesting result is the negative correlation between the proportion of the “Grid” and “Circuitous” (Pearson correlation=-0.646), revealing their opposite effects on the F1 score.

To further explore the functions of our newly defined spatial homogeneity, we performed the principal component analysis (PCA) on the 11-dimension vector representation of URN. The first principal component PC1 encoded small average degree, large circuitry, dendricity, and explained 48% of data variability (**Supplementary Table 11**). PC1 was defined as Street-Network Disconnectedness index (SNDi) and investigated in the previous studies^{34,39}. PC1 was shown to be positively correlated with circuitry and dendricity (the fraction of bridge edges and dead-end edges) and negatively related to the average degree. A URN with large SNDi included rivers, hills, and gated communities with cul-de-sacs while a URN with small SNDi was composed of grid blocks. In **Fig. 2e**, we visualized the PC1 and F1 scores for all testing URN samples in 30 cities and observed the stunning correlation: F1 score was negatively correlated to SNDi (Pearson correlation=-0.484). In other words, a URN with a larger SNDi was less predictable. This negative relationship was more significant in the USA (Pearson correlation=-0.563) than Europe, Asia (Pearson correlation=-0.269, -0.430) (**Supplementary Fig. 9**). In fact, cities in the US had a relatively short history of population agglomeration⁴⁰, and their road networks were built regularly under strict urban planning and land ordinance policies, which could be traced back to the grid plan in Philadelphia since the early 18th century⁴¹. In contrast, most megacities in Europe and Asia (e.g., London, Beijing) experienced longer urbanization periods, during which both the top-down planning policy and self-organization simultaneously carved the urban prototype⁴². As illustrated

in **Figs. 2f-h**, Chicago has a prevalent distribution of grid-like blocks, while Paris and Singapore are occupied by roads with irregular shapes of blocks.

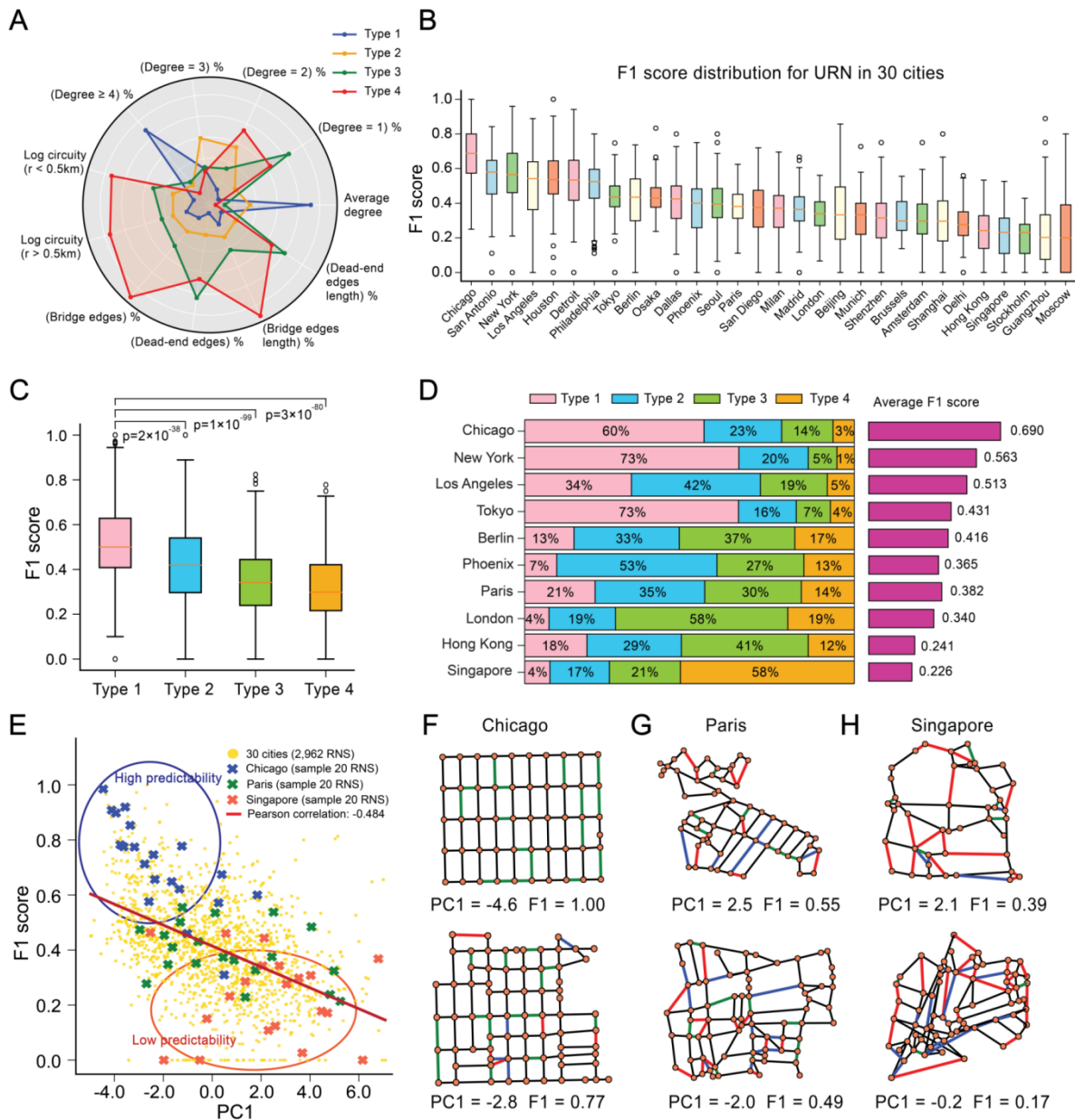


Fig. 2. Relationship between URN homogeneity and URN type, SNDi. (A) Coordinates of centroids of four types of URN clustered by using k -means algorithm. (B) Boxplots of F1 scores for testing URN samples in thirty cities. (C) Boxplots of F1 scores for the four types we obtained in (A). (D) Type compositions and the average F1 scores of URN in ten representative cities. (E) Relationship between the F1 score and the PC1 value for all URNs. F1 score decreases when the PC1 value increases, suggesting a compelling connection between interpretable PC1 values and uninterpretable F1 scores. (F), (G), (H) Link prediction results. Green links denote true positive (links exist in both reality and prediction), red links denote false positive (links exist in prediction but not reality), and blue links denote false negative (links exist in reality but not prediction).

Connections with network statistics

We found that spatial homogeneity of a URN showed revealing associations with several conventional network statistics, such as road length and average betweenness. Understanding these connections helps to make an early assessment of the spatial homogeneity of a URN before the GNN training processes. These network statistics are also powerful indicators of several traffic functionalities, such as traffic commute time and delay⁴³ and road safety⁴⁴. We expected our homogeneity measure could also serve as a bridge to associate the traffic functionalities and contribute to urban planning. As an example, we first investigated the interconnections between spatial homogeneity and average degree, betweenness (**Fig. 3a**). We found that cities with a high average degrees and low average betweenness (e.g., New York, Chicago, San Antonio) had higher F1 scores than other cities (e.g., Phoenix, Shanghai, Moscow). Significant distinctions of F1 scores were observed when the 30 cities were evenly distributed into two groups based on their values of betweenness and degree (**Figs. 3b,c**). Low betweenness and high degree cities had high spatial homogeneity (P-values<0.001 under one-sided t-tests). These results aligned with the intuition that an intersection with more road segments was likely to receive more neighborhood information via the message passing mechanism in GNN, resulting in high predictability. In contrast, high average betweenness cities were anticipated to have low predictability. This was because these cities had high betweenness road segments (such as bridges) that attracted large proportions of short-path flows, stood out among their neighboring road segments, and were therefore hard to predict based on the neighboring context.

Connections with social-economic indicators

We also examined the connections amid the spatial homogeneity and Gross Domestic Production (GDP) and populations, which were extensively surveyed in enormous socio-economic studies^{45,46}. As the growth of URN fluctuated during decades, we employed population growth (PG) which was defined as the ratio of population in *Year 2* over *Year 1* to measure the increase of the population from *Year 1* to *Year 2* (**Supplementary Fig. 10**). PG for all 30 cities was calculated based on the population data spanning from 1950 to 2020 (**Supplementary Note 4**). We uniformly classified each city as one of the four categories based on its GDP and PG values. For example, London (GDP=634 billion dollars, PG(1950→2020)=1.140) ranked respectively in the first half, the latter half among 30 cities in terms of GDP and PG(1950→2020), so we classified London into “High GDP & Low PG” class. In **Figs. 3d-g**, we perceived that during different time intervals, the cities in “High GDP & Low PG” class had significantly higher prediction accuracy than the other three classes of cities (P-values<0.050 under one-sided t-tests). Moreover, we found that all “High GDP & Low PG” cities (London, Paris, New York, Los Angeles, Chicago, Philadelphia, Osaka) were in developed countries and we named them as “advanced cities”. Our interpretation of this phenomenon is that “advanced cities” invested much more in road network planning annually so that their road networks were more standard and predictable. Besides, the low PG in an “advanced city” revealed that this city had already experienced rapid population growth and entered a stable period, and the tendency of road network expansion was weak and consequently more predictable.

We also performed regression analysis between the spatial homogeneity and fifteen measures from four categories: social-economic factors, road network scale metrics, road density metrics, and network topology metrics (see full data in **Supplementary Tables 15,16**). We conducted linear regression with the explanatory variable as one of these fifteen factors and the response variable as the average F1 score for the same city. The R-squared values (**Fig. 3h**) for the regression, the

P-values (**Fig. 3i**) for the coefficients of fifteen factors under two-sided t-tests were calculated to demonstrate the statistics significance. It is worthy to note that R-squared value reflects the amount of variance explained by a single socio-economic or network metric, telling whether it is sufficient to use a single variable to predict the F1 score. Whereas the P-value illustrates whether the introduction of the single variable is significantly better than the null model with the intercept only, revealing the necessity of this variable to fit the F1 score (**Fig. 3i**). The P-value classifies decisive factors that are related to the F1 score (homogeneity of the URN) and are useful to track changes of F1 scores under dynamic socio-economic and network contexts along decades.

In **Figs. 3h,i**, we recognize that PG was more relevant than the population itself in determining URN homogeneity (R-squares: 0.115 VS 0.048, P-values: 0.071 VS 0.243), implying that the population growth was a stronger indicator of the urbanization stage, when human activities greatly affected URN homogeneity, than population. The F1 score was found to be associated with GDP and irrelevant to airport passenger flow. Moreover, the F1 score was positively related to road network metrics whereas road density metrics were weak predictors (R-squares<0.130). Note that the land area was not sufficient to solely estimate the F1 score (R-square=0.071) but was significantly related to F1 score (P-value<0.001), revealing that the urban coverage affected but did not fully determine URN homogeneity. Finally, the average degree and betweenness were also appropriate URN homogeneity predictors (R-squares>0.290, P-values<0.003).

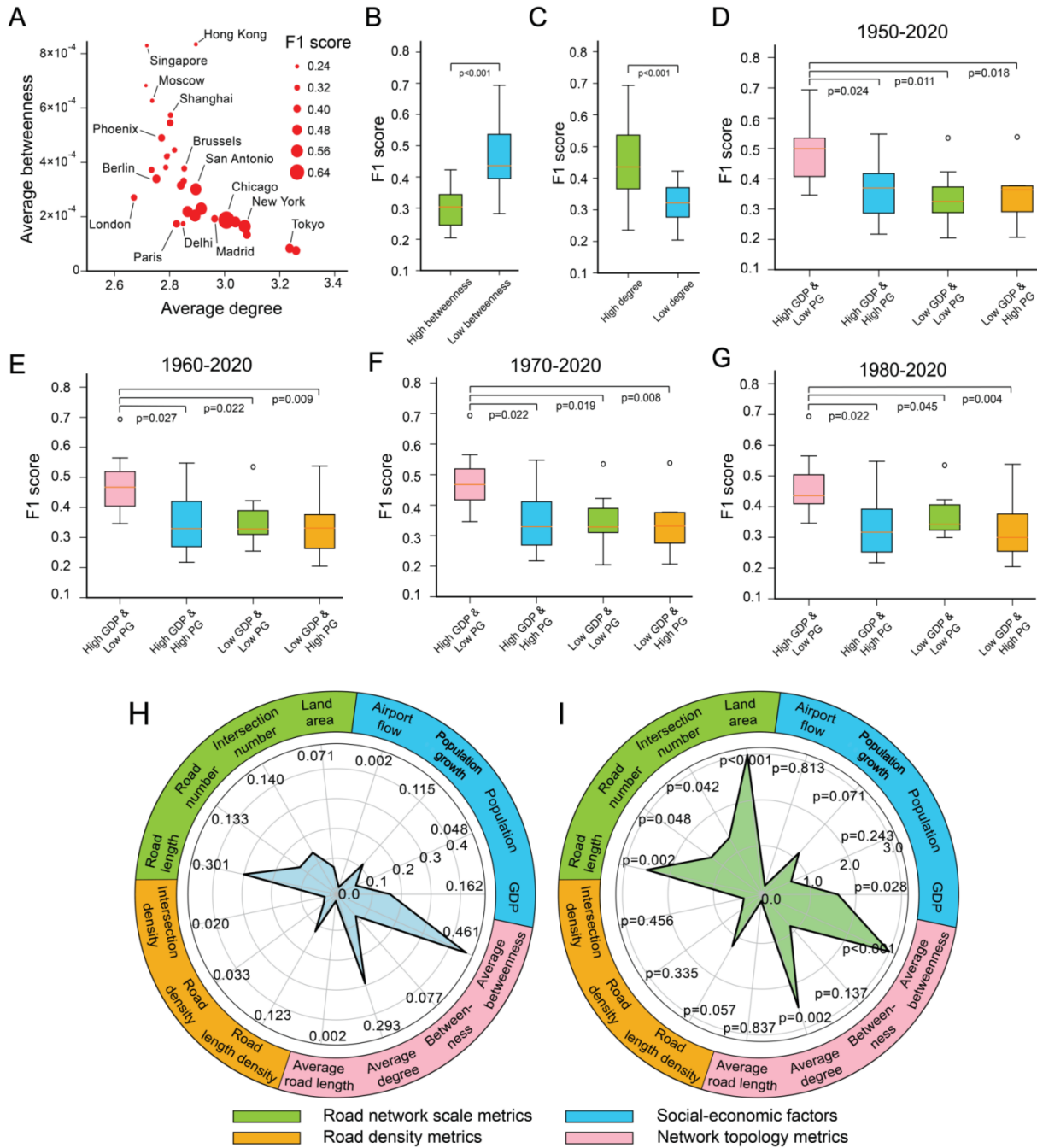


Fig. 3. Association between URN homogeneity and network metrics, social-economic factors. (A) Average F1 scores for 30 cities under average degree and average betweenness coordinates. F1 score tends to be high when the average degree is high and the average betweenness is low. (B), (C) Boxplots of F1 scores for different cities defined by betweenness and degree. (D), (E), (F), (G) Boxplots of F1 scores for different cities defined by their GDP, and population growth (PG). Four figures have different time periods when computing PG. (H) R-squared values for linear regression with a single explanatory variable when the response variable is the F1 score. (I) P-values for the explanatory variables in the linear regression the same as (H). To better visualize small P-values, we replaced $p < 0.001$ with $p = 0.001$ and drew the wind plot based on $-\log(p)$.

Inter-city homogeneity

We surveyed the inter-city URN homogeneity by transferring the URN knowledge learned from GNN across various cities, which was notable evidence for future urban knowledge transfer tasks. Here, urban knowledge transfer originates from transfer learning^{47,48} that applies the multi-granularity data and multi-modularity labels from one city to urban tasks in another city to address with the data and label scarcity issues for the latter city⁴⁹. It has extensive applications and computational models, such as human mobility data generation⁵⁰, spatial-temporal traffic prediction⁵¹, cross-city point of interest (POI) recommendation⁵². However, these approaches were task-specific and lacked a universal discussion of whether it was reliable to perform urban knowledge transfer between any pair of cities in the world. Owing to the strong dependence of socio-economic activities on the road network, which is the backbone of urban space, measuring the homogeneity of road networks across cities assists in evaluating the inter-city transferability of these activities.

We performed the cross-city link prediction (trained GNN models on city *A* and tested on city *B* across 30 cities) and implemented hierarchical clustering on these cities based on their transferability. The average F1 scores for training and testing cities were presented in **Figs. 4a,b**, and the City Homogeneity Transfer Matrix (CHTM) was exhibited in **Fig. 4c**. Note that CHTM was not symmetric: the F1 score obtained by training on city *A* and testing on city *B* differed from the F1 score when swapping *A* and *B*. In CHTM, a high F1 score block was situated at the top-left corner (training: from Milan to Seoul; testing: from Chicago to Los Angeles). For this block, most training cities were historical European cities (Milan, London, Paris, etc.) or USA cities (Los Angeles, Chicago, New York, etc.), whereas testing cities were primarily USA cities (10 out of 13), revealing that URN patterns in the USA were sufficiently covered by these training cities. This result was consistent with the history that the American urban planning style was inspired originally from European cities. The second observation was that there were four city clusters from the testing side: “USA”, “Asia(c)”, “Asia(w)”, “Europe” (**Figs. 4a,c**). In general, “USA” type cities had the highest F1 scores, and “Europe” type cities, all from Europe, were not so predictable. The other two types with weak prediction performance were “Asia(c)” type and “Asia(w)” type. “Asia(c)” type cities were heavily affected by Chinese culture whereas “Asia(w)” cities had active connections with the western world. For instance, Ginza, an international commercial area in Tokyo, experienced a “model of modernization” urban reconstruction designed by Thomas Waters in the late 19th century⁵³, and was portrayed as a less representative area in oriental cities but resembled Chicago by traveler Isabella L. Bird⁵⁴. Collectively speaking, American cities were accurately planned and constructed and therefore predictable, while cities in Europe and Asia were shaped simultaneously by intricate historical and modern factors. Another interesting observation was that the transferring from Milan to Seoul achieved higher F1 scores than remaining cities (**Figs. 4b,c**). We deduced that if a city contained multiple sub-structures and had a large spatial coverage, it was likely that the topological features learned from this city were applicable to other cities. In this case, we reasoned that these cities had excellent road network “diversity”. Most Asian cities had deficient “diversity” as they did not exert significant impacts worldwide in urban planning as cities in Europe and the USA. When encoding each city by a five-dimension vector composed of conventional network metrics and computing the inter-city similarity by cosine vector angles, we found the similarity values were sensitive to the normalization setting and did not reveal any interpretable road network pattern across cities (**Figs. 4d,e**), demonstrating the weakness of conventional network metrics in exploration inter-city URN topological patterns.

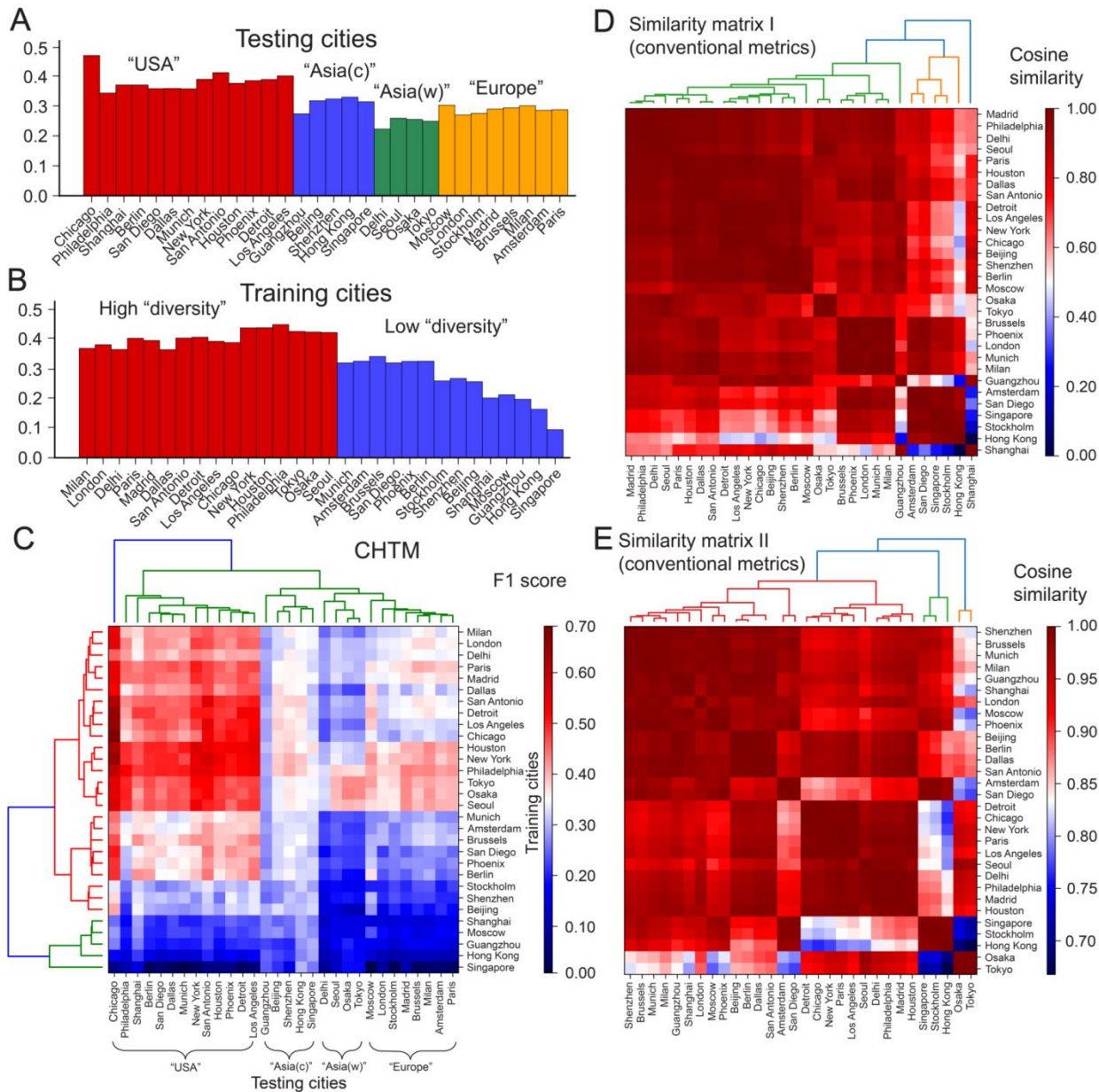


Fig. 4. The City homogeneity transfer matrix (CHTM) and city similarity matrix using conventional network metrics. (A), (B) Average F1 scores for testing cities and training cities. **(C)** CHTM. Each cell denotes the average F1 score on URN in the testing city when learning the URN pattern from a training city. **(D)** City similarity matrix I (normalized by dividing the value over the maximal value). **(E)** City similarity matrix II (normalizing values linearly to 0 and 1).

Spatial distribution of inter-city homogeneity

Next, we study the transferring performance on each local city region (1km by 1km) from a historical point of view (**Fig. 5**). For instance, when the R-GCN model was trained on Chicago, New York and tested on Los Angeles (LA), the south and west of downtown area achieved better prediction performance than both downtown, northern, and eastern LA, implying that southern and western LA were more consistent with Chicago and New York in terms of road network style (**Figs. 5a,b**). The early settlement in Los Angeles concentrated on the downtown whose road networks had been shaped by complicated forces for long. After the 1880s, rapid urban expansion converted the farmland into urban areas, along the direction of current Interstate-10 and Interstate-110, under a united municipal zoning ordinance which had a far-reaching influence on contemporary American cities, resulting in the high predictability of these “new” areas⁵⁵.

Contrasting results appear for a historical city such as Osaka. We found that the road networks in downtown Osaka could be well predicted by the model trained on Tokyo whereas the prediction performance for the surrounding areas is not very good (**Fig. 5c**). The reason is that cultural centripetal force and short spatial distance helped Osaka and Tokyo form a tight social-economic (including road network planning) connection, since the period when downtown Osaka was populated. However, the “new” populated urban land which was far from downtown Osaka was mostly constructed after the 1870s, when both the domestic and international urban planning mode exerted influence. As a result, road networks in downtown Osaka are weakly captured by London and New York (**Fig. 5d, Supplementary Fig. 11c**). Seoul had a stronger connection with Osaka than London and New York before the 1870s and therefore achieved better prediction performance in downtown Osaka (**Supplementary Fig. 11d**).

Another key finding was the reclaimed land in Tokyo. We noticed that URNs in the reclaimed area at the coast of Tokyo Bay were better captured by the road network pattern learned from Chicago, New York, London, and Paris than the broad area in the western part of Tokyo (**Figs. 5e,f** and **Supplementary Figs. 11e,f**). Administrations in Tokyo had a long history of turning Tokyo bay into usable land via landfill technologies. The “reclaimed land” marked in **Figs. 5e,f** were mostly filled after 1987 for residence, exhibition, amusement purposes⁵⁶. Road networks on these artificial islands were “modern”, not following the traditional road network styles as inland Tokyo, and shared some similarities with the road networks in other international cities.

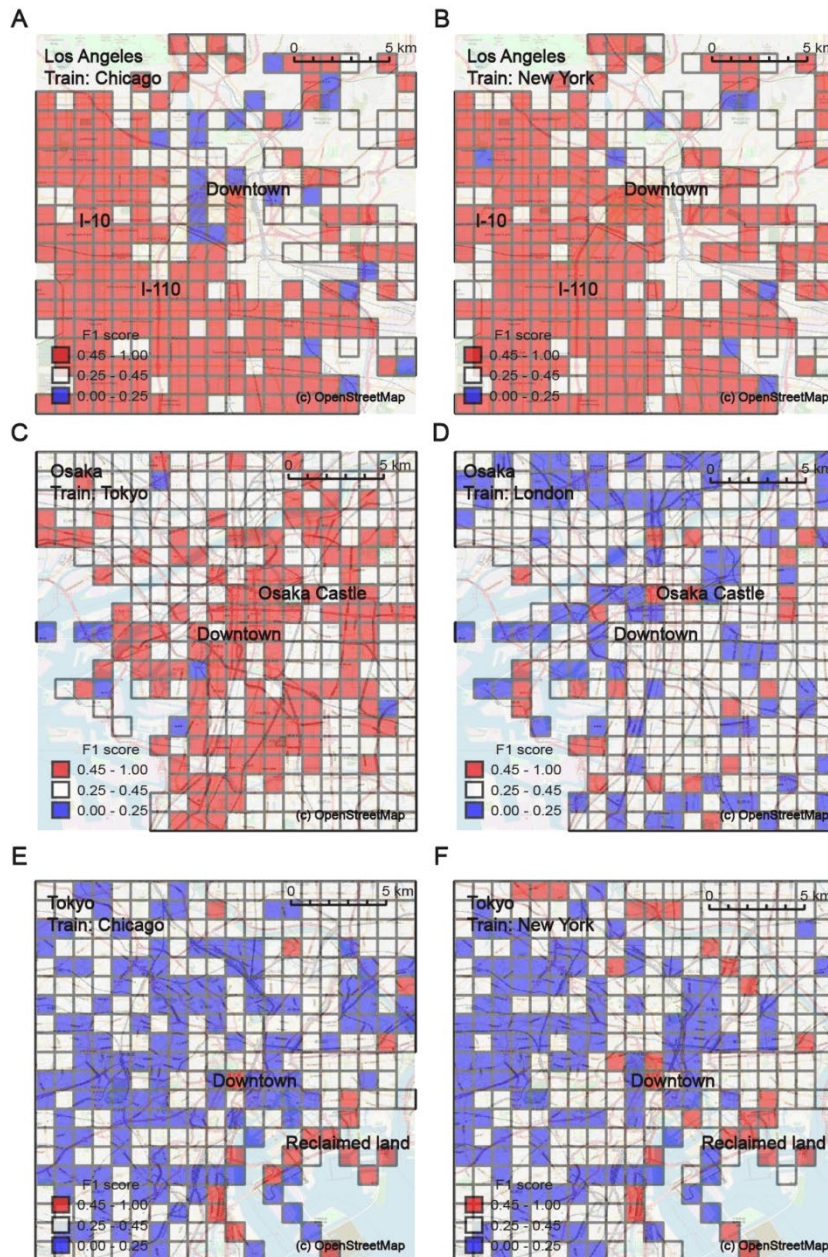


Fig. 5. The spatial distribution of inter-city prediction results. Red, white, blue were used to present high, medium, low F1 scores. **(A), (B)** Maps of Los Angeles (LA). **(C), (D)** Maps of Osaka. Road network types in downtown Osaka were well captured by Tokyo other than London. **(E), (F)** Maps of Tokyo. Reclaimed lands near Tokyo Bay had high F1 scores.

DISCUSSION

We proposed an advanced GNN-based metric that established our understanding of the inner-city and inter-city spatial homogeneity of urban road networks. URN homogeneity measures the similarity in different urban regions⁵⁷, non-linearly integrating the information of both the local and global network structures that jointly determine the efficiency and resilience of traffic network⁵⁸, the direction and velocity of cascading failures⁵⁹. This novel metric leverages the power of GNN for encoding the complicated URN structure pattern and capturing multi-scale node dependencies. It also shows interesting connections with previous road network attributes (such as road network type, SNDi) and classic network metrics (such as degree, betweenness) and captures extra URN similarity information. In addition, we noticed that the URN homogeneity was associated with economic activities (GDP) and population growth, pointing toward a broader infrastructure-society interaction⁶⁰. Compared with the previous metrics, our URN homogeneity has the exclusive functionality of quantifying the asymmetric similarity between two cities, providing a prerequisite for multiple urban transfer learning tasks^{49,50,52} as well as city similarity discoveries⁶¹.

The self-similarity of a complex system was extensively studied as Fractals in mathematics⁶², physics^{19,63}, and ecology⁶⁴. Fractal is the object whose parts are analogous to the whole system and has implications of theories about network dynamics such as the percolation process²⁸, which serves as a successful approach connecting the structure and dynamics in the complex network. These successes motivated us to quantify the URN homogeneity and further unravel the interplay between URN structure and dynamics, where most transportation network models made strong assumptions about the optimality of people's route choices. Our GNN-based models and potential variants are promising approaches to understand the universal pattern of traffic dynamics. Besides, the GNN-based link prediction model has other practical usages. It allows urban planners to understand which road segments are more likely to exist based on current URN contexts so that these road segments can have high priorities in road network planning. Another application is geospatial database development: map editors can infer missing links and predict the future growth of road networks, using prediction results and other data (e.g., vehicle GPS trajectory, satellite images).

Although GNN encodes intricate node dependencies from large URN data, the prediction performance degrades when GNN goes deeper, resulting from the vanishing gradient⁶⁵ and over-smoothing⁶⁶ issues in the model training stage. The overall prediction performance could be improved using more advanced learning architectures and training algorithms in the future. In addition, the link prediction reliability of URN in each city, which is affected by the size of selected urban areas (20km by 20km), node merging threshold (30m), train-test split ratio (75%, 25%), link hidden percentage (20%) (**Supplementary Note 1**), should be also considered. In fact, the parameter rigorousness in road network research is a common challenge. In the study of SNDi^{34,39}, the authors set the node merging threshold to 20 meters after comparing it with 14 meters. In our work, we defined it as 30 meters after checking the node merging results in New York and London (**Supplementary Figs. 3, 4**). Comprehensive parameter sensitivity tests and a unified criterion tailored to different road network structures help to reach more robust prediction outcomes across distinct cities.

Taken together, the URN homogeneity metric sheds light on network structure-dynamic investigations and a variety of urban transferring tasks. The association study between URN homogeneity and multiple network metrics, social-economic factors could also be applied to early

assessment of URN homogeneity and infrastructure-society interaction surveys while the asymmetric CHTM reveals the interplays between cities from different continents. In the future, comprehensive road network, urban traffic data (such as road hierarchy, traffic flow) with sufficient granularity would promote more accurate quantifications of the URN homogeneity. In practice, user-friendly URN homogeneity computing packages are also favorable to increase the machine learning implementation efficiency in various urban planning and transportation practices. This work is a significant advance in understanding the URN structural relationships building on pioneering work^{5-7,67} in the fields of road network structure and dynamics in recent years.

MATERIALS AND METHODS

Datasets description

All datasets in this work are accessible publicly. We utilized the OSMnx package⁶⁸ to download the road network data from OpenStreetMap (OSM), which was widely used for academic purposes^{15,58,68}. To investigate the URN homogeneity for distinct cities, we chose 30 cities from the USA, Europe, and Asia (**Supplementary Table 1**). Each city was sampled the urban area with a coverage of 20km by 20km (**Supplementary Fig. 1**) and the size of each URN was defined as 1km by 1km (**Supplementary Fig. 2**). We also set the training and testing sample ratio to 3:1 (**Supplementary Table 2**). To deal with the “duplicate node problem”, we implemented a node merging algorithm and verified the merging performance on road networks in New York and London (**Supplementary Figs. 3, 4**). The aggregated network statistics for URN in 30 cities are displayed in **Supplementary Table 3**. In addition, we collected the social indicator data (GDP, population, airport flow) which was used in the association analysis (**Supplementary Table 15**).

Link prediction of URN

Our machine learning task was the link prediction on URN, where we sampled 80% of links and predicted the presence of the rest 20% (**Supplementary Note 2**). The link prediction on URN was a binary classification, consisting of an encoder (which generates a vector representation for each node, **Fig. 1b**) and a decoder (which calculates the connecting strength between two nodes, **Fig. 1c**). We utilized the R-GCN as the encoder, DistMult as the decoder. In R-GCN, the information propagation from layer l to $(l + 1)$ was:

$$h_i^{l+1} = \tanh\left(\sum_{r \in R} \sum_{j \in N_i^r} \frac{1}{c_i^r} W_r^l h_j^l\right) + W_0^l h_i^l \quad (1)$$

where h_i^l, h_i^{l+1} were the node representations of node i at layer l and $(l + 1)$, $r \in R$ was the link relation, N_i^r denoted the adjacent node set of node i with the relation r . c_i^r was a normalization constant, and W_r^l was the learnable matrix about the relation r in the l -th layer. The link relation r was defined from the relative angle: we evenly divided 360° into eight direction intervals (N, S, E, W, NE, NW, SE, SW, where N, S, E, W indicate north, south, east, west), resulting in eight types of relations. Note that we defined h_i^0 as the initial embeddings of node i concatenated with the normalized latitude and longitude. In DistMult, the scoring strength $s(i, j)$ for node i and j was:

$$s(i, j) = h_i^T W_d h_j \quad (2)$$

where h_i, h_j were the final node embeddings, W_d was the learnable diagonal matrix. Finally, we used the sigmoid function to transform the range of scoring strength to $(0, 1)$:

$$\sigma(s(i, j)) = \frac{1}{1 + \exp(-s(i, j))} \quad (3)$$

In the decoding stage, we added the “acute angles” and “intersecting link” avoidance improvements: once both sigmoid connecting strengths for two pairs of nodes exceeded the threshold δ :

$$\sigma(s(i_1, j_1)) > \sigma(s(i_2, j_2)) \geq \delta \quad (4)$$

then we predicted that the first link (i_1, j_1) existed, the second link (i_2, j_2) did not exist, if the “relative angles” between the two links was less than a certain acute angle or they intersected within the link (**Supplementary Fig. 5**). The intuition was that road networks were embedded in urban space and such phenomena rarely happened. We named the R-GCN model with improved DistMult as R-GCN*. Next, we used Adam optimizer⁶⁹ minimising the cross-entropy loss:

$$\text{minimise}_{W_r, W_d} - \frac{1}{(1+\omega)|E|} \sum_{(i,j) \in \tau} (y \log(\sigma(s(i,j))) + (1-y) \log(1 - \sigma(s(i,j)))) \quad (5)$$

where $y = 1$, $y = 0$ denoted the positive and negative links. Since the dataset contained more negative links than positive links, we randomly sampled the negative links under the negative: positive ratio as $\omega = 5:1$. We built a graph neural network with three layers and each layer had 50 hidden neurons. We trained the model for 10 epochs with the learning rate of 0.001. The threshold to determine the final sigmoid connecting strength was 0.61. In the inner-city prediction, we trained separate models for different cities whereas in the inter-city prediction, we trained on city *A* and tested on city *B*. To compare the performance of our model, we also implemented five other GNN models (Node2vec⁷⁰, Struc2vec⁷¹, GraphSage⁷², Spectral GCN⁷³, Graph Attention Network (GAT)⁷⁴, **Supplementary Note 2**) to benchmark the prediction. The running time of both training and testing for 30 cities was ~15 mins (R-GCN, R-GCN*), ~15 mins (Spectral GCN), ~90 mins (GAT), ~100 mins (Node2vec), ~250 mins (Struc2vec), ~300 mins (GraphSage) under the Windows system with 8-core i7 Intel CPUs, implying that R-GCN, R-GCN* are the most efficient ones and comprehensive road network homogeneity computation takes acceptable running time in a personal computer.

Definition of URN homogeneity

URN homogeneity describes the similarity between the part and whole road networks. The link prediction utilizes the global road network information to predict the hidden links in the local road network. In this way, a URN with high homogeneity tends to be predictable. In addition, the F1 score measures the prediction performance for the unbalanced dataset. Therefore, for each URN, we defined the URN homogeneity level as the F1 score of link prediction, for each city, we defined the city URN homogeneity as the average F1 scores of all URNs in this city.

Association analysis

We performed a comprehensive association analysis between the URN homogeneity and URN type, SNDi, network metrics, and social-economic indicators. We followed the work³⁴ to obtain the URN type and SNDi. In particular, we computed 11 measurements (**Supplementary Table 6**) from 3 aspects (node degree, circuitry, dendricity) using the NetworkX Python package (<https://networkx.org/>). Here, node degree quantified the number of road segments joining an intersection, circuitry was the ratio of shortest network distance to the Euclidean distance between the start and end node, while dendricity indicated the impact of each road on URN connectivity complemented by dead-end edges, bridge edges. Next, we tried distinct numbers k of clusters and noticed under the case of $k = 4$, partitions of URN had the best interpretability (see URN visualization in **Supplementary Tables 7-10**). In addition, we conducted the PCA on these vectors (**Supplementary Table 11**), using the PC1 to define the SNDi, which represented the sprawl of URN³⁴. We computed other network metrics (road network scale metrics, social-economic factors, road density metrics), collected social-economic data (GDP, population, airport flow) for each city

(**Supplementary Table 15**). All variables were fed into a single variable linear regression model to test the linear relationship with F1 scores, which was used for an early assessment of F1 scores.

REFERENCES AND NOTES

1. Sun, L., Axhausen, K. W., Lee, D.-H. & Huang, X. Understanding metropolitan patterns of daily encounters. *Proc. Natl. Acad. Sci. U. S. A.* **110**, 13774–13779 (2013).
2. Xu, Y., Olmos, L. E., Abbar, S. & González, M. C. Deconstructing laws of accessibility and facility distribution in cities. *Sci Adv* **6**, (2020).
3. Snellen, D., Borgers, A. & Timmermans, H. Urban Form, Road Network Type, and Mode Choice for Frequently Conducted Activities: A Multilevel Analysis Using Quasi-Experimental Design Data. *Environment and Planning A: Economy and Space* vol. 34 1207–1220 (2002).
4. Zhan, X., Ukkusuri, S. V. & Rao, P. S. C. Dynamics of functional failures and recovery in complex road networks. *Phys Rev E* **96**, 052301 (2017).
5. Li, D. *et al.* Percolation transition in dynamical traffic network with evolving critical bottlenecks. *Proc. Natl. Acad. Sci. U. S. A.* **112**, 669–672 (2015).
6. Saberi, M. *et al.* A simple contagion process describes spreading of traffic jams in urban networks. *Nature Communications* vol. 11 (2020).
7. Çolak, S., Lima, A. & González, M. C. Understanding congested travel in urban areas. *Nat. Commun.* **7**, 10793 (2016).
8. Foley, J. A. Global Consequences of Land Use. *Science* vol. 309 570–574 (2005).
9. Depersin, J. & Barthelemy, M. From global scaling to the dynamics of individual cities. *Proc. Natl. Acad. Sci. U. S. A.* **115**, 2317–2322 (2018).
10. Strano, E. *et al.* The scaling structure of the global road network. *R Soc Open Sci* **4**, 170590 (2017).
11. Molinero, C., Murcio, R. & Arcaute, E. The angular nature of road networks. *Sci. Rep.* **7**, 4312 (2017).
12. Porta, S., Crucitti, P. & Latora, V. The network analysis of urban streets: A dual approach. *Physica A: Statistical Mechanics and its Applications* vol. 369 853–866 (2006).
13. Kalapala, V., Sanwalani, V., Clauset, A. & Moore, C. Scale invariance in road networks. *Phys. Rev. E Stat. Nonlin. Soft Matter Phys.* **73**, 026130 (2006).
14. Crucitti, P., Latora, V. & Porta, S. Centrality measures in spatial networks of urban streets. *Phys. Rev. E Stat. Nonlin. Soft Matter Phys.* **73**, 036125 (2006).
15. Kirkley, A., Barbosa, H., Barthelemy, M. & Ghoshal, G. From the betweenness centrality in street networks to structural invariants in random planar graphs. *Nat. Commun.* **9**, 2501 (2018).
16. Jiang, B. & Claramunt, C. Topological Analysis of Urban Street Networks. *Environment and Planning B: Planning and Design* vol. 31 151–162 (2004).
17. Louf, R. & Barthelemy, M. A typology of street patterns. *J. R. Soc. Interface* **11**, 20140924 (2014).
18. Lee, M., Barbosa, H., Youn, H., Holme, P. & Ghoshal, G. Morphology of travel routes and the organization of cities. *Nat. Commun.* **8**, 2229 (2017).
19. Barabási, A.-L. & Stanley, H. E. *Fractal Concepts in Surface Growth*. (Cambridge University Press, 1995).
20. Cheng, F., Kovács, I. A. & Barabási, A.-L. Publisher Correction: Network-based prediction of drug combinations. *Nat. Commun.* **10**, 1806 (2019).

21. Jalili, M., Orouskhani, Y., Asgari, M., Alipourfard, N. & Perc, M. Link prediction in multiplex online social networks. *R Soc Open Sci* **4**, 160863 (2017).
22. Dong, Y. *et al.* Link Prediction and Recommendation across Heterogeneous Social Networks. *2012 IEEE 12th International Conference on Data Mining* (2012) doi:10.1109/icdm.2012.140.
23. Ren, Y., Ercsey-Ravasz, M., Wang, P., González, M. C. & Toroczkai, Z. Predicting commuter flows in spatial networks using a radiation model based on temporal ranges. *Nat. Commun.* **5**, 5347 (2014).
24. Teney, D., Liu, L. & Van Den Hengel, A. Graph-Structured Representations for Visual Question Answering. *2017 IEEE Conference on Computer Vision and Pattern Recognition (CVPR)* (2017) doi:10.1109/cvpr.2017.344.
25. Wu, N., Zhao, X. W., Wang, J. & Pan, D. Learning Effective Road Network Representation with Hierarchical Graph Neural Networks. *Proceedings of the 26th ACM SIGKDD International Conference on Knowledge Discovery & Data Mining* (2020) doi:10.1145/3394486.3403043.
26. Colizza, V., Barrat, A., Barthélemy, M. & Vespignani, A. The role of the airline transportation network in the prediction and predictability of global epidemics. *Proc. Natl. Acad. Sci. U. S. A.* **103**, 2015–2020 (2006).
27. Olden, J. D., Lawler, J. J. & Poff, N. L. Machine learning methods without tears: a primer for ecologists. *Q. Rev. Biol.* **83**, 171–193 (2008).
28. Chayes, L. Aspects of the Fractal Percolation Process. *Fractal Geometry and Stochastics* 113–143 (1995) doi:10.1007/978-3-0348-7755-8_6.
29. Freeman, L. C. A Set of Measures of Centrality Based on Betweenness. *Sociometry* vol. 40 35 (1977).
30. Holme, P. CONGESTION AND CENTRALITY IN TRAFFIC FLOW ON COMPLEX NETWORKS. *Advances in Complex Systems* vol. 06 163–176 (2003).
31. Gao, S., Wang, Y., Gao, Y. & Liu, Y. Understanding Urban Traffic-Flow Characteristics: A Rethinking of Betweenness Centrality. *Environment and Planning B: Planning and Design* vol. 40 135–153 (2013).
32. Strano, E., Nicosia, V., Latora, V., Porta, S. & Barthélemy, M. Elementary processes governing the evolution of road networks. *Sci. Rep.* **2**, 296 (2012).
33. OpenStreetMap. <https://www.openstreetmap.org/>.
34. Barrington-Leigh, C. & Millard-Ball, A. A global assessment of street-network sprawl. *PLoS One* **14**, e0223078 (2019).
35. Stanfield, Z., Coşkun, M. & Koyutürk, M. Drug Response Prediction as a Link Prediction Problem. *Sci. Rep.* **7**, 40321 (2017).
36. Yang, Yang, Y., Chawla, N., Sun, Y. & Hani, J. Predicting Links in Multi-relational and Heterogeneous Networks. *2012 IEEE 12th International Conference on Data Mining* (2012) doi:10.1109/icdm.2012.144.
37. Schlichtkrull, M. *et al.* Modeling Relational Data with Graph Convolutional Networks. *The Semantic Web* 593–607 (2018) doi:10.1007/978-3-319-93417-4_38.
38. Yang, B. *et al.* Embedding Entities and Relations for Learning and Inference in Knowledge Bases. Preprint at <https://arxiv.org/abs/1412.6575> (2015).
39. Barrington-Leigh, C. & Millard-Ball, A. Global trends toward urban street-network sprawl. *Proceedings of the National Academy of Sciences* vol. 117 1941–1950 (2020).
40. Shapiro, V. W. & Rosenwaike, I. Population History of New York City. *The History Teacher* vol. 6 633 (1973).
41. Hammack, D. C., Weighley, R. F. & Lukacs, J. Philadelphia: A 300-Year History. *The*

- American Historical Review* vol. 89 878 (1984).
42. Barthelemy, M., Bordin, P., Berestycki, H. & Gribaudi, M. Self-organization versus top-down planning in the evolution of a city. *Sci. Rep.* **3**, 2153 (2013).
 43. Ewing, R., Pendall, R. & Chen, D. Measuring Sprawl and Its Transportation Impacts. *Transportation Research Record: Journal of the Transportation Research Board* vol. 1831 175–183 (2003).
 44. Marshall, W. E. & Garrick, N. W. Does street network design affect traffic safety? *Accid. Anal. Prev.* **43**, 769–781 (2011).
 45. Kumm, M., Taka, M. & Guillaume, J. H. A. Gridded global datasets for Gross Domestic Product and Human Development Index over 1990–2015. *Scientific Data* vol. 5 (2018).
 46. Immerzeel, W. W. *et al.* Importance and vulnerability of the world's water towers. *Nature* **577**, 364–369 (2020).
 47. Dai, W., Yang, Q., Xue, G.-R. & Yu, Y. Boosting for transfer learning. *Proceedings of the 24th international conference on Machine learning - ICML '07* (2007) doi:10.1145/1273496.1273521.
 48. Han, J., Pei, J. & Kamber, M. *Data Mining: Concepts and Techniques*. (Elsevier, 2011).
 49. Wei, Y., Zheng, Y. & Yang, Q. Transfer Knowledge between Cities. *Proceedings of the 22nd ACM SIGKDD International Conference on Knowledge Discovery and Data Mining* (2016) doi:10.1145/2939672.2939830.
 50. He, T. *et al.* What is the Human Mobility in a New City: Transfer Mobility Knowledge Across Cities. *Proceedings of The Web Conference 2020* (2020) doi:10.1145/3366423.3380210.
 51. Yao, H., Liu, Y., Wei, Y., Tang, X. & Li, Z. Learning from Multiple Cities: A Meta-Learning Approach for Spatial-Temporal Prediction. *The World Wide Web Conference on - WWW '19* (2019) doi:10.1145/3308558.3313577.
 52. Ding, J., Yu, G., Li, Y., Jin, D. & Gao, H. Learning from Hometown and Current City. *Proceedings of the ACM on Interactive, Mobile, Wearable and Ubiquitous Technologies* vol. 3 1–28 (2019).
 53. Vivers, M. *An Irish Engineer: The Extraordinary Achievements of Thomas J Waters and Family in Early Meiji Japan and Beyond*. (2013).
 54. Bird, I. L. *Unbeaten Tracks in Japan: An Account of Travels in the Interior Including Visits to the Aborigines of Yezo and the Shrines of Nikkō and Isé*. (1880).
 55. Whittemore, A. H. Zoning Los Angeles: a brief history of four regimes. *Planning Perspectives* vol. 27 393–415 (2012).
 56. Endoh, T. Historical Review of Reclamation Works in Tokyo Port Area. *Journal of Geography (Chigaku Zasshi)* vol. 113 534–538 (2004).
 57. Liu, Y., Zhao, K. & Cong, G. Efficient Similar Region Search with Deep Metric Learning. *Proceedings of the 24th ACM SIGKDD International Conference on Knowledge Discovery & Data Mining* (2018) doi:10.1145/3219819.3220031.
 58. Ganin, A. A. *et al.* Resilience and efficiency in transportation networks. *Sci Adv* **3**, e1701079 (2017).
 59. Zhao, J., Li, D., Sanhedrai, H., Cohen, R. & Havlin, S. Spatio-temporal propagation of cascading overload failures in spatially embedded networks. *Nat. Commun.* **7**, 10094 (2016).
 60. Chandra, A. & Thompson, E. Does public infrastructure affect economic activity? *Regional Science and Urban Economics* vol. 30 457–490 (2000).
 61. Currid, E. & Williams, S. Two Cities, Five Industries: Similarities and Differences within and between Cultural Industries in New York and Los Angeles. *Journal of Planning*

Education and Research vol. 29 322–335 (2010).

62. Falconer, K. *Techniques in Fractal Geometry*. (Wiley, 1997).

63. Nakayama, T., Yakubo, K. & Orbach, R. L. Dynamical properties of fractal networks: Scaling, numerical simulations, and physical realizations. *Reviews of Modern Physics* vol. 66 381–443 (1994).

64. Halley, J. M. *et al.* Uses and abuses of fractal methodology in ecology. *Ecology Letters* vol. 7 254–271 (2004).

65. He, K., Zhang, X., Ren, S. & Sun, J. Deep Residual Learning for Image Recognition. *2016 IEEE Conference on Computer Vision and Pattern Recognition (CVPR)* (2016) doi:10.1109/cvpr.2016.90.

66. Chen, D. *et al.* Measuring and Relieving the Over-Smoothing Problem for Graph Neural Networks from the Topological View. *Proceedings of the AAAI Conference on Artificial Intelligence* vol. 34 3438–3445 (2020).

67. Loder, A., Ambühl, L., Menendez, M. & Axhausen, K. W. Understanding traffic capacity of urban networks. *Sci. Rep.* **9**, 16283 (2019).

68. Boeing, G. A Multi-Scale Analysis of 27,000 Urban Street Networks: Every US City, Town, Urbanized Area, and Zillow Neighborhood. doi:10.31235/osf.io/hmhts.

69. Diederik P., Jimmy B. Adam: A Method for Stochastic Optimization. Preprint at <https://arxiv.org/abs/1412.6980> (2014).

70. Grover, A. & Leskovec, J. node2vec: Scalable Feature Learning for Networks. *KDD 2016*, 855–864 (2016).

71. Ribeiro, Leonardo F.R., *et al.* struc2vec: Learning Node Representations from Structural Identity. *KDD 2017*, 385–394 (2017)

72. Kipf, T. N., & Welling, M. Semi-supervised classification with graph convolutional networks. Preprint at <https://arxiv.org/abs/1609.02907> (2016).

73. Hamilton, W., Ying, Z. & Leskovec, J. Inductive Representation Learning on Large Graphs. *Adv. Neural Inf. Process. Syst.* **30**, 1024–1034 (2017).

74. Petar V., Guillem C. Graph Attention Networks. Preprint at <https://arxiv.org/abs/1710.10903> (2018).

Acknowledgements: We thank the discussion with Prof. Suresh Rao in Purdue University about comparison between URN homogeneity index and other network metrics.

Author contributions: J.X., S.V.U., J.M. proposed the question; J.X., N.J., S.L., Q.P., J.M. designed the research; N.J. implemented the GNN models; S.L. and Q.P. performed the association analysis; N.J., J.X. conducted inter-city analysis; J.X. and J.M. drew the figures; J.X., S.V.U and J.M. analyzed results and wrote the paper.

Competing interests: The authors declare no competing interests.

Data and materials availability: The road network data for 30 cities were collected via OSMnx Python package developed by Dr. Geoff Boeing. Both the road network data, social-economic data, source codes for training, testing, inter-city homogeneity results are available at the online data warehouse: <https://github.com/jiang719/road-network-predictability.git>.